Chinese Chemical Letters 34 (2023) 107085

Contents lists available at ScienceDirect

Chinese Chemical Letters

journal homepage: www.elsevier.com/locate/cclet

Tuning host-guest binding model by different intramolecular alkyl chain lengths in tripodal hosts: An evidence on structure control supramolecular interactions

Zheng-Hua Zhang[a], You-Ming Zhang[a,b,*], Wen-Juan Qu[a], Bingbing Shi[a], Hong Yao[a], Tai-Bao Wei[a,*]

[a] Key Laboratory of Eco-environmental Polymer Materials of Gansu Province, College of Chemistry and Chemical Engineering, Northwest Normal University, Lanzhou 730070, China
[b] Gansu Natural Energy Research Institute, Lanzhou 730046, China

ARTICLE INFO

Article history:
Received 31 July 2021
Revised 28 December 2021
Accepted 29 December 2021
Available online 4 January 2022

Keywords:
Host-guest recognition
Supramolecular interactions
Fluorescent
Intramolecular alkyl chain
Aggregation induced emission

ABSTRACT

Supramolecular chemistry has received considerable attention in host-guest recognition. The structure-response relationship of host-guest recognition system is a meaningful issue. Herein, a series of tripodal nitrogen mustard derivatives (**TMs**) have been developed in this paper. By rationally design the intramolecular alkyl chain lengths of host, the host-guest binding model have been successfully tuned, which underwent a transformation from π-π to multiple hydrogen bonds. This process enhances the host-guest binding force and recognition efficiency.

Detection of nitroaromatic compounds (NACs) such as trinitrotoluene (TNT) and picric acid (PA) has attracted wide attentions [1–4]. Widespread application of PA may not only cause serious health problems, also results in the severe environment pollution [5,6]. Therefore, it is necessary to design methods to improve the detection sensitivity and selectivity of PA [7–9].

How to improve the selectivity in host-guest recognition is an important issue for supramolecular chemistry [10,11]. The design and application of novel supramolecular host for efficiently recognition target guest through non-covalent forces is one of the key trends [12–14]. It can be seen that improving the host-guest binding force is challenging. The host structure is one of the key factors which influence the binding property of the host-guest recognition system. It is a very meaningful topic to improve the selectivity and sensitivity of the host-guest system through rational investigate the structure-response relationship of host.

Moreover, in recent years, applications based on aggregation induced emission (AIE) sensors have fascinated more and more attention [15–17]. AIE also provides a new idea in fluorescent probes [18–20]. How to improve the recognition efficiency of AIE through regulating the molecule structures is also an interesting theme.

In view of these and our long-term research foundation in fluorescence chemosensors, in order to study the influence of different host structures on the host-guest recognition properties, herein, we have designed and synthesized three tripodal small molecule probes **TM**, **TM2** and **TM4** with different intramolecular alkyl chains which linked binding sites of the hosts. Interestingly, when the alkyl chain was different, the host-guest binding model as well as binding force was also different. The supramolecular interactions could be regulated from π-π stacking to multiple hydrogen bonds, meanwhile, the recognition efficiency has been improved.

The **TMs** (**TM**, **TM2** and **TM4**) were synthesized and fully characterized by IR, NMR and HRMS (Schemes S1, S2 and Figs. S8, S9, S16-S21 in Supporting information). The AIE properties of **TMs** were primary explored by the fluorescence characteristics of DMSO/H_2O mixed solution with different water components. In the DMSO/H_2O binary system, DMSO was used as a good solvent for **TMs**, while water was a poor solvent for **TMs**. In the **TM** system, as the water fraction (f_w) increased, the fluorescence emission intensity of **TM** gradually increased and reached a maximum

* Corresponding authors.
E-mail addresses: zhangnwnu@126.com (Y.-M. Zhang), weitaibao@126.com (T.-B. Wei).

https://doi.org/10.1016/j.cclet.2021.12.077
1001-8417/

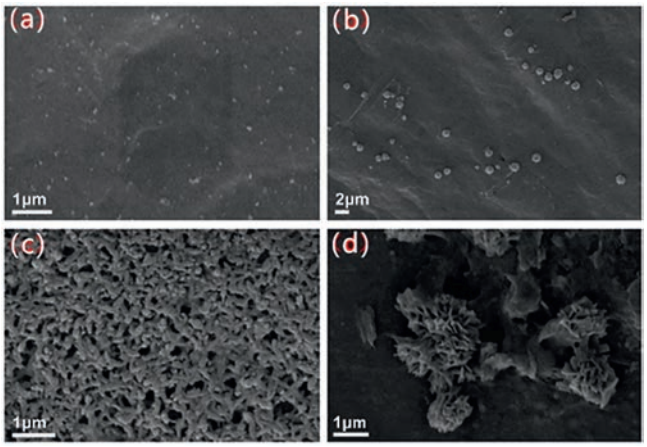

Fig. 1. SEM images of (a) **TM2** in DMSO, (b) **TM2** in DMSO–H_2O (4:1), (c) **TM2** in DMSO–H_2O (1:9) and (d) **TM2**-PA.

at 50% water fraction (Fig. S1a in Supporting information), while, which were 20%, 40% for **TM2** and **TM4**, respectively (Figs. S1b and c in Supporting information). In order to verify the AIE process, the morphologies of the **TMs** with different moisture content were investigated by SEM. As shown in Fig. 1, after drying the corresponding **TM** solutions in air and got the SEM images of them, the **TM2** obtained from the pure DMSO shown irregular particles structures, while with the increase of water content, obvious aggregation observed. The SEM images of **TM** and **TM4** were similar to **TM2** (Figs. S13 and S14 in Supporting information). This suggests that the main mechanism of AIE effect of **TMs** compounds is due to water-induced agglomeration, which limits the dissipation of excited state energy caused by intramolecular rotation. This is consistent with the classical RIM theory [21].

Afterward, as shown in Fig. 2b and Fig. S3 (Supporting information), the fluorescent recognition performances of **TMs** for nitroaromatic compounds (NACs) were primarily explored by adding a series of NACs, including picric acid, 2-nitrophenol, 3-nitrophenol, 4-nitrophenol, 2,4-dinitrophenol, 2-nitrobenzoic acid, 3-nitrobenzoic acid, 4-nitrobenzoic acid, 4-nitrobenzaldehyde, 2-nitroaniline, 3-nitroaniline, 4-nitroaniline and 4-nitrotoluene into **TMs** solution separately. As a result, **TMs** could selectively recognize PA by fluorescent response. In the fluorescence titration experiments of **TMs** with PA, as shown in Fig. 2a and Fig. S2 (Supporting information), the fluorescence spectra of **TM**, **TM2** and **TM4** exhibited intense emission λ_{max} at 502, 470 and 430 nm, respectively. While, the fluorescence quenching occurred with the gradually increasing of PA. Additionally, the PA specific selectivity of sensor **TMs** over other miscellaneous NACs was carefully investigated *via* control experiments under competitive condition. Fig. 2c and Fig. S4 (Supporting information) showed that the coexist competition NACs could not cause any significant interference for the **TMs** sensing to PA.

In order to investigate the influence of different structures of **TMs** on the sensitivity of PA detection, the detection limit (LOD), quenching constant (K_{SV}) and corresponding binding constant (K_a) were studied in detail. The LOD was calculated by way of $3\delta/S$ method [22]. From the experiments, it was found that the LOD of PA were observed to be 8.0×10^{-8} mol/L for **TM**, 5.7×10^{-8} mol/L for **TM2** and 3.1×10^{-8} mol/L for **TM4** respectively (Fig. S5 in Supporting information). K_{SV} was studied by Stern-Volmer (SV) equation $I_0/I = 1 + K_{SV}[Q]$ [23]. I_0 and I were the fluorescence intensities in the absence and presence of PA and [Q] was concentration of quencher PA. K_{SV} was the Stern-Volmer rate constant, which was calculated conveniently by the slope of the plot of I_0/I *vs.* [Q]. Fig. S6 (Supporting information) showed the corresponding K_{SV} of **TM**, **TM2** and **TM4** were estimated to be 2.3×10^4 L/mol, 5.5×10^4 L/mol and 6.0×10^4 L/mol respectively. The *K*a values for **TMs-**PA complex were directly related to the stability of these complexes. It was calculated by fluorescence titration experiment and obtained by non-linear fitting [24]. We performed the data fitting for **TMs**:PA 1:1 complex and calculated the binding constant. The corresponding *K*a was evaluated to be 2.9×10^4 L/mol, 5.0×10^4 L/mol and 7.8×10^4 L/mol for **TM**, **TM2** and **TM4** respectively (Fig. S7 and Eq. S1 in Supporting information). As summarized in Table 1, the **TMs** can sensitively detect PA at the ppb level and the **TM4** shows the highest sensitivity. The quenching efficiency of PA was also the highest for **TM4** which had the longest intramolecular alkyl chain among **TMs**. Meanwhile, the **TM4** also had the highest binding capacity.

Table 1
The stoichiometry, LOD, *K*a and K_{sv} of **TMs** with PA.

Compounds	Chain length in **TMs**	LOD (mol/L)	*K*a (L/mol)	K_{SV} (L/mol)
TM	0	8.0×10^{-8}	2.9×10^4	2.3×10^4
TM2	2	5.7×10^{-8}	5.0×10^4	5.5×10^4
TM4	4	3.1×10^{-8}	7.8×10^4	6.0×10^4

In order to understand the influence of molecular structure on supramolecular interactions and recognition efficiency, the FT-IR, ^{1}H NMR titration, ESI-MS and SEM were carried out. The ^{1}H NMR titration was used to check the host-guest binding mode of **TMs** and PA in DMSO–d_6 solution. As shown in Fig. 3a, addition of PA to **TM** resulted in upshift of the proton signals H1-H7 of **TM** and downshift of the proton signals H_a of PA, which clearly reflected that **TM** and PA undergo π-π and van der Waals force interactions to form the supramolecular complex [25]. However, as showed in Fig. 3c, according to ^{1}H NMR titration of **TM4** and PA, an obvious downshift was inspected for the chemical shift of the H1-H10 atoms in **TM4**. The results showed that the **TM4** binding the PA through N – H···O and C – H···O multiple hydrogen bonds interactions and forming a stable complex with PA [26,27]. Analogously, the proton signals H1-H7 of **TM2** were shifted downfield gradually upon the addition of PA, which indicated that the strong N – H···O and C – H···O multiple hydrogen bonds were formed between the **TM2** with PA (Fig. 3b). Moreover, the proton signal of PA underwent significant upshift when interacting with **TM2** and **TM4**, while it only slightly shifted to downfield when combined with **TM**. For the **TM**, the quenching of the fluorescence would be related to the change of electron cloud density between **TM** and PA *via* the π-π stacking [28]. However, for the **TM2** and **TM4**, the electrons were transferred from **TM2** and **TM4** to electron-deficient PA by the stronger multiple hydrogen bonds interactions. This difference of the host-guest recognition models was attributed to the different intramolecular alkyl chains in the molecular structure of host (Fig. 3). Therefore, the interaction between host and guest should undergo a transition from π-π stacking and der Waals force interactions to hydrogen bonds as the linker increased from 0 to 4 methylene. Meanwhile, the magnitude of chemical shift on the host and guest increased significantly. These showed that the hydrogen bonding between host and guest increased with the increase of linker length. Therefore, when the linker was one and three methylene, the interaction between host and guest should be hydrogen bonding, that was, the hydrogen on the host should move to the lower field, and the hydrogen on the guest should move to the higher field. However, when the linker was one and three methylene, the magnitude of the chemical shift of hydrogen on the host and guest was smaller and larger than that when the linker was two methylene groups, respectively.

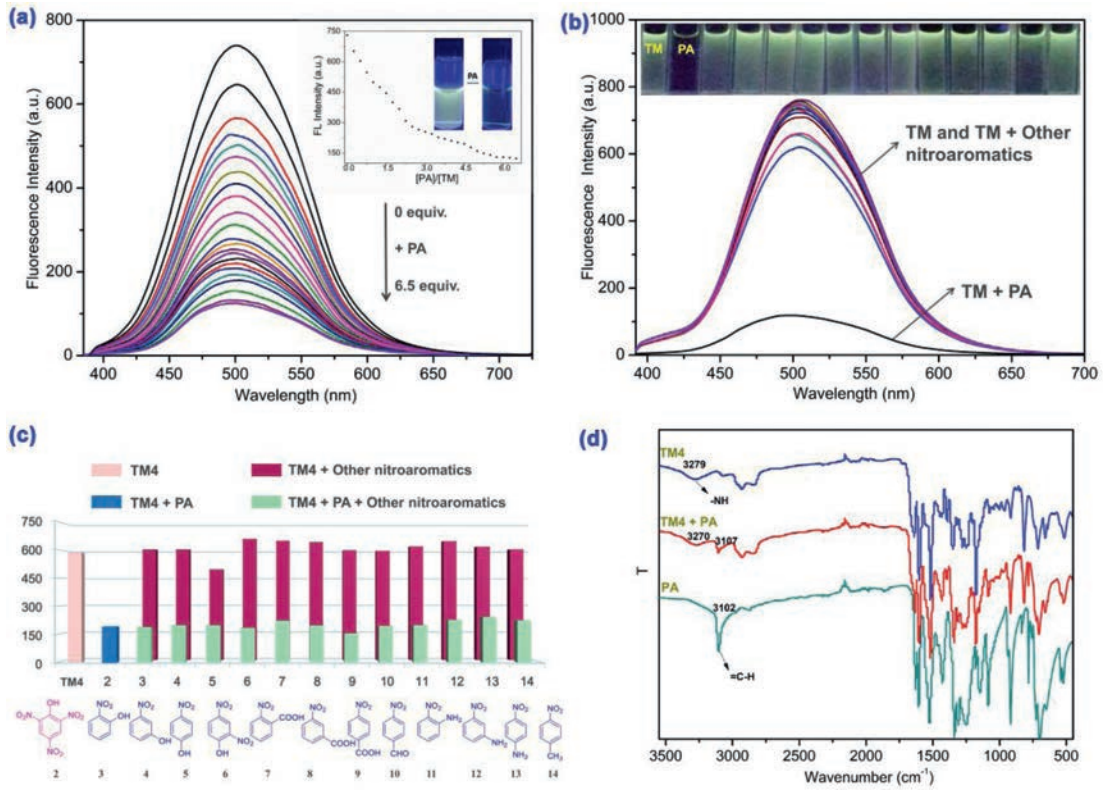

Fig. 2. Emission spectra of **TM** (2×10^{-5} mol/L, DMSO/H_2O (1:1, v/v) binary solution) in (a) fluorescence titration of with PA and (b) various nitroaromatic compounds (6.5 equiv.). (c) Fluorescence emission value of the **TM4** (2×10^{-5} mol/L, DMSO/H_2O (3:2, v/v) binary solution) to PA (2.55 equiv.) in the presence of various nitroaromatic compounds, (d) IR spectra of **TM4**, **TM4-PA** and PA.

The FT-IR spectra of PA, **TMs** and **TMs** + PA complex were carried out to further understand the interaction process. For the PA, the stretching vibration absorption peak of =C–H appeared on benzene ring at 3102 cm^{-1}. The peak located at 3279 cm^{-1} was attributed to the stretching vibration of -NH in the **TM4** (Fig. 2d). When PA is added to the **TM4**, the -NH stretching vibration absorption peak shifted to 3270 cm^{-1} and the =C–H stretching vibration absorption peak shifted to 3107 cm^{-1}. Similarly, in the mixture of **TM** and PA, the -NH characteristic absorption peak shifted from 3204 to 3198 cm^{-1} and the =C–H characteristic absorption peak shifted from 3102 to 3104 cm^{-1} (Fig. S8 in Supporting information). For the **TM2** + PA complex, the -NH characteristic absorption peak shifted from 3275 to 3264 cm^{-1} and the =C–H characteristic absorption peak shifted from 3102 to 3106 cm^{-1} (Fig. S9 in Supporting information). The results also showed that the formation of N – H···O and C – H···O multiple hydrogen bonds.

Simultaneously, these inferences were also supported by the ESI-MS spectra of **TMs** and PA. As displayed in the Fig. S10 (Supporting information), the peaks at 1194.1992 and 1661.2079 were attributed to the formation of $[\mathbf{TM} + PA + CH_3OH]^+$ and $[\mathbf{TM} + 3PA + CH_3CN]^+$ complexes. Fig. S11 (Supporting information) showed that the peaks at 1263.2738, 763.6787 and 1743.2889 were consistent with $[\mathbf{TM2} + PA + H_2O\text{-}H]^+$, $[\mathbf{TM2} + 2PA + 2(CH_3CN)\text{–}3H]^{2+}$ and $[\mathbf{TM2} + 3PA + CH_3CN\text{–}2H]^+$. The peaks at 484.4731, 1600.3857 and 1828.3833 were ascribed to the formation of $[\mathbf{TM4} + PA + 3(CH_3CN)]^{3+}$, $[\mathbf{TM4} + 2PA + CH_3CN]^+$ and $[\mathbf{TM4} + 3PA + CH_3CN\text{-}H]^+$ complexes respectively (Fig. S12 in Supporting information). All of above indicated that with the increase of PA, **TMs** and PA formed the stabilized host-guest complex from 1:1 to 1:3.

The morphology of **TMs** before and after combining PA was also characterized by SEM. For the **TM** after added to the PA, a large number of fibrous morphologies with a length of several microns and a diameter of several nanometers were appeared, which a flower-like shape was formed through self-assembly (Fig. S15a in Supporting information). We found the hierarchical micro-flowers formed by self-assembly of lots of nanosheets while the PA added to the **TM2** (Fig. 1d). And the complex of **TM4** and PA could form the small flower-like structure by nanosheets and nanorods. These changes in morphologies clearly showed that **TMs** and PA have formed new complexes (Fig. S15b in Supporting information).

In short, in order to study the structure-response relationship, we have designed and synthesized three chemosensors (**TMs**) with different intramolecular alkyl chains. The corresponding results suggested that with the increasing of the length of linker alkyl chain, the host-guest binding model was changed from π-π interactions to multiple hydrogen bonds. The binding model showed directly influence on the recognition efficiency for these PA sensors. As a result, among **TM**, **TM2** and **TM4**, **TM4** has the longest intramolecular alkyl chain, which exhibited higher detection selectivity, stronger quenching constant and binding constant. The **TM4** could sensitively detect PA at the ppb level. This result indicated that multiple hydrogen bonds host-guest binding model was more efficient than π-π stacking model. Therefore, we realized the regulation of host-guest recognition model and efficiency through adjusting the host structure. The present strategy is enlightening, and we expect it could provide a new idea and method to improve the host-guest recognition efficiency by rationally adjusting the host molecular structure.

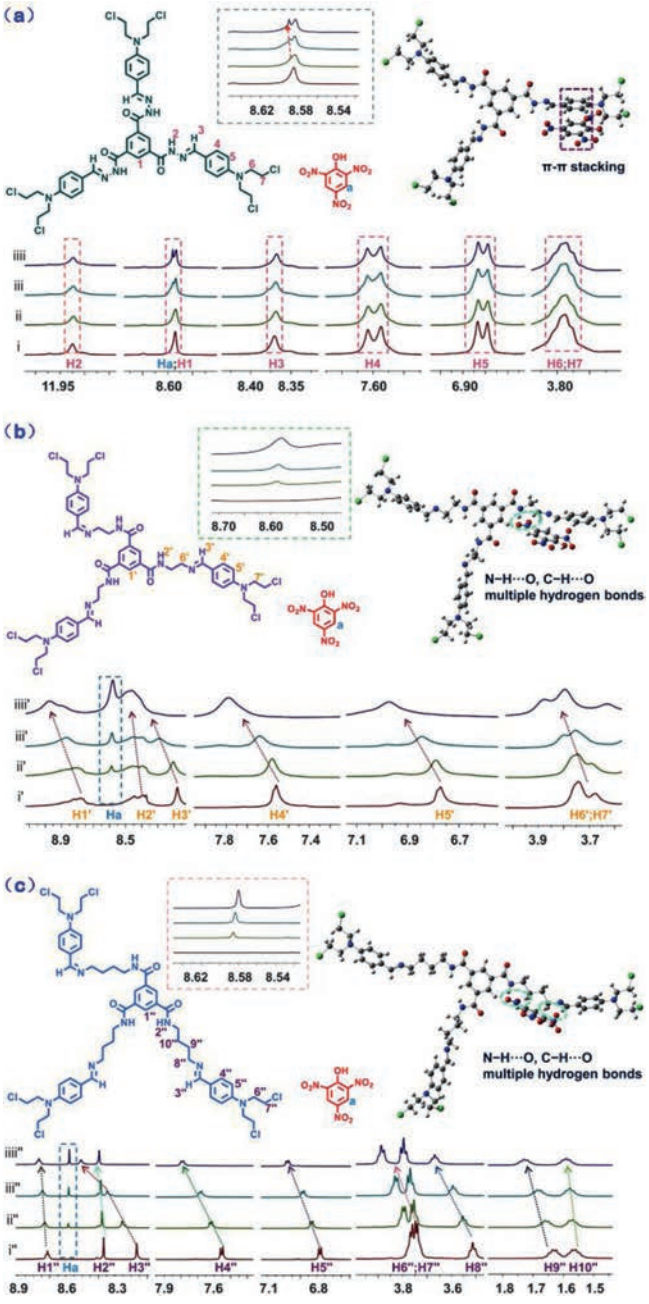

Fig. 3. Partial ^{1}H NMR spectra changes (DMSO–d_6). (a) (i) **TM**, (ii) **TM** + 0.5 equiv. PA, (iii) **TM** + 1.0 equiv. PA, (iiii) **TM** + 2.0 equiv. PA; (b) (i′) **TM2**, (ii′) **TM2** + 0.5 equiv. PA, (iii′) **TM2** + 1.0 equiv. PA, (iiii′) **TM2** + 2.0 equiv. PA; (c) (i″) **TM4**, (ii″) **TM4** + 0.5 equiv. PA, (iii″) **TM4** + 1.0 equiv. PA, (iiii″) **TM4** + 2.0 equiv. PA.

Declaration of competing interest

The authors declare that they have no known competing financial interests or personal relationships that could have appeared to influence the work reported in this paper.

Acknowledgments

The authors gratefully acknowledge the support from the National Natural Science Foundation of China (Nos. 22165027, 22061039, 22001214), Key R & D program of Gansu Province (No. 21YF5GA066) and Gansu Provincial Department of Education: Excellent Postgraduate "Innovation Star" Project (No. 2021CXZX-184).

Supplementary materials

Supplementary material associated with this article can be found, in the online version, at doi:10.1016/j.cclet.2021.12.077.

References

[1] Y. Liang, L. Xu, F. Qu, et al., Polym. Chem. 10 (2019) 4818–4824.
[2] Z.H. Fu, Y.W. Wang, Y. Peng, Chem. Commun. 53 (2017) 10524–10527.
[3] M. Ansari, R. Bera, S. Mondal, D. Neeladri, ACS Omega 4 (2019) 9383–9392.
[4] N.G. Khaligh, M.R. Johan, Nano 13 (2018) 1830006.
[5] H. Zhou, J. Li, M.H. Chua, et al., Polym. Chem. 5 (2014) 5628–5637.
[6] D.C. Santra, M.K. Bera, P.K. Sukul, S. Malik, Chem. Eur. J. 22 (2016) 2012–2019.
[7] Z.Y. Li, Z.Q. Yao, R. Feng, et al., Chin. Chem. Lett. 32 (2021) 3095–3098.
[8] S. Mondal, P. Bairi, S. Das, A.K. Nandi, Chem. Eur. J. 24 (2018) 5591–5600.
[9] S. Xing, Q. Bing, H. Qi, et al., ACS Appl. Mater. Inter. 9 (2017) 23828–23835.
[10] H. Duan, Y. Li, Q. Li, et al., Angew. Chem. Int. Ed. 59 (2020) 10101–10110.
[11] Y. Sakata, M. Tamiya, M. Okada, S. Akine, J. Am. Chem. Soc. 141 (2019) 15597–15604.
[12] Y. Huo, Z. He, C. Wang, et al., Chem. Commun. 57 (2021) 1413–1429.
[13] B. Qin, Z. Yin, X. Tang, et al., Prog. Polym. Sci. 100 (2020) 101167.
[14] C. Xu, L. Xu, X. Ma, Chin. Chem. Lett. 29 (2018) 970–972.
[15] Y.Y. Chen, X.M. Jiang, G.F. Gong, et al., Chem. Commun. 57 (2021) 284–301.
[16] J.J. Li, H.Y. Zhang, G. Liu, et al., Adv. Optical Mater. 9 (2021) 2001702.
[17] L. Xu, Z. Wang, R. Wang, et al., Angew. Chem. Int. Ed. 59 (2020) 9908–9913.
[18] L. Zhang, Y. Sun, Y. Jiang, et al., Chin. Chem. Lett. 31 (2020) 2428–2432.
[19] T. Feng, X. Li, J. Wu, C. He, C. Duan, Chin. Chem. Lett. 31 (2020) 95–98.
[20] S. Wang, C.H. Zhang, P. Zhang, et al., Anal. Methods 13 (2021) 2030–2036.
[21] G.X. Feng, B. Liu, Small 12 (2016) 6528–6535.
[22] Analytical Methods Committee, Analyst 112 (1987) 199–204.
[23] M.C. Rong, L.P. Lin, X.H. Song, et al., Anal. Chem. 87 (2015) 1288–1296.
[24] L. Xu, R. Wang, W. Cui, et al., Chem. Commun. 54 (2018) 9274–9277.
[25] S. Kasthuri, K. Shiv, S. Raviteja, et al., Appl. Surf. Sci. 481 (2019) 1018–1027.
[26] Y.M. Zhang, Q.Y. Yang, X.Q. Ma, et al., J. Phys. Chem. A 124 (2020) 9811–9817.
[27] T. Xiao, L. Zhou, X.Q. Sun, et al., Chin. Chem. Lett. 31 (2020) 1–9.
[28] N. Yan, J. Song, F. Wang, et al., Chin. Chem. Lett. 30 (2019) 1984–1988.